

## Electronic Supplementary Information

### Experimental Section

#### Chemicals and materials

Cobalt nitrate hexahydrate ( $\text{Co}(\text{NO}_3)_2 \cdot 6\text{H}_2\text{O}$ ), urea ( $\text{CH}_4\text{N}_2\text{O}$ ), ammonium chloride ( $\text{NH}_4\text{Cl}$ ), ammonium fluoride ( $\text{NH}_4\text{F}$ ), yttrium chloride hexahydrate ( $\text{YCl}_3 \cdot 6\text{H}_2\text{O}$ ), ammonium chloride- $^{15}\text{N}$  ( $^{15}\text{NH}_4\text{Cl}$ - $^{15}\text{N}$ ), potassium nitrate- $^{15}\text{N}$  ( $\text{K}^{15}\text{NO}_3$ - $^{15}\text{N}$ ), potassium sulfate ( $\text{K}_2\text{SO}_4$ ), sulfamic acid, phosphoric acid, p-aminobenzenesulfonamide, N-(1-Naphthyl) ethylenediamine dihydrochloride, potassium sodium tartrate,  $\text{NaNO}_2$  and Nessler's reagent and potassium nitrate ( $\text{KNO}_3$ ) were purchased from Aladdin (Shanghai, China). Hydrochloric acid and ethanol ( $\text{C}_2\text{H}_5\text{OH}$ ) were purchased from Beijing Chemical Works.

#### Synthesis of Y-Co(OH)F/CF and Co(OH)F/CF

A one-step hydrothermal method with some modifications was applied to prepare Y-Co(OH)F/CF catalysts. First, the cleaned Cu foam ( $2 \times 4 \text{ cm}^2$ ) was submerged in an aqueous solution with 30 mL of the following: 5 mmol  $\text{Co}(\text{NO}_3)_2 \cdot 6\text{H}_2\text{O}$ , 5 mmol urea, 400 mg  $\text{NH}_4\text{F}$  and 0.05 mmol  $\text{YCl}_3 \cdot 6\text{H}_2\text{O}$ . After being transferred into a 50 mL Teflon autoclave, the solution was heated at  $120 \text{ }^\circ\text{C}$  for 12 hours. In the end, deionized water was used to clean up the generated Y-Co(OH)F/CF sample, and then dried at  $50 \text{ }^\circ\text{C}$  in the oven. With the exception of adding 0.05 mmol  $\text{YCl}_3 \cdot 6\text{H}_2\text{O}$ , the Co(OH)F/CF counterpart was synthesized similarly to Y-Co(OH)F/CF.

#### Materials Characterization

The morphology of Y-Co(OH)F/CF was investigated with a Zeiss Gemini 500 scanning electron microscope. Images from transmission electron microscopy (TEM), high-resolution transmission electron microscopy (HRTEM) and high-angle annular dark-field scanning transmission electron

microscopy (HAADF-STEM) were recorded on a TalosS-FEG. Using a PANalytical X'Pert-PRO X-ray diffractometer with Cu K radiation, the powder X-ray diffraction(XRD) patterns of Y-Co(OH)F/CF were examined. The X-ray photoelectron spectrometer (XPS) manufactured by Kratos Analytical was used for studying the chemical valence states and elemental makeup of Y-Co(OH)F/CF. On a Bruker Avance NEO 600 NMR spectrometer, the spectra of  $^1\text{H}$  NMR were analyzed.

### **Electrochemical $\text{NO}_3\text{RR}$ measurements**

A three-electrode setup was used for the electrochemical technique, and the CHI 660 electrochemical workstation was used for all electrochemical tests. A Pt foil, Y-Co(OH)F/CF ( $1 \times 1 \text{ cm}^2$ ), and SCE were used in the three-electrode setup as the counter electrode, working electrode and reference electrode, respectively. 35 mL of 0.5 M  $\text{K}_2\text{SO}_4$  was placed separately to the H-cell's anode and cathode chambers for the nitrate reduction tests. From  $-0.7$  to  $-1.5 \text{ V}$  (vs. SCE), linear sweep voltammetry (LSV) curves were captured at a scan rate of  $10 \text{ mV s}^{-1}$ . After the LSV curves had stabilized, the 35 ml of 0.5 M  $\text{K}_2\text{SO}_4$  was swapped out for 0.5 M  $\text{K}_2\text{SO}_4$  with  $200 \text{ mg L}^{-1}$   $\text{KNO}_3\text{-N}$ . Pass argon gas through the electrolyte for 30 minutes, and two hours of chronoamperometry (i-t) investigates were conducted at various potentials with a 500 rpm mixing rate. Nitrate and ammonia concentrations were determined by UV-VIS spectroscopy. Electrochemical impedance spectroscopy (EIS) measurements were performed in a 0.5 M  $\text{K}_2\text{SO}_4$  aqueous solution with  $200 \text{ mg L}^{-1}$  of  $\text{NO}_3\text{-N}$  at  $-1.3 \text{ V}$  (vs. SCE) with frequency from 0.1 Hz to 100 kHz and an amplitude of 5 mV.

### **Determination of $\text{NO}_3\text{-N}$**

First, the electrolyte was withdrawn and diluted to 5 ml according to the measurement range after

the two hours of testing. Then 0.1 mL of HCl solution (1 M) and 0.01 mL of 0.8 wt% sulfamic acid solution are then added to the electrolyte in sequence. After a thorough shake, the color was produced in dark for ten minutes. The absorbance was measured by UV-Vis spectrophotometry in the wavelength range of 200 nm and 300 nm. The final absorbance of  $\text{NO}_3^-$ -N was calculated by the following formula:  $A = A_{220\text{nm}} - 2A_{275\text{nm}}$ . The calibration curve is created by measuring the absorbance corresponding to the reference concentration of  $\text{KNO}_3$  solution.

### **Determination of $\text{NO}_2^-$ -N**

First, 5 mL of deionized water was used to dissolve 0.02 g of N-(1-naphthyl) ethylenediamine dihydrochloride and 0.4 g of p-aminobenzene sulfonamide. Add 1 mL of phosphoric acid (= 1.70 g  $\text{mL}^{-1}$ ) next to act as a color developing agent. For 20 minutes, 5 mL of diluted electrolyte was combined with 0.1 mL of color developing agent. UV-Vis spectrophotometry was used to get the peak absorption spectrum at a wavelength of 540 nm. By using  $\text{NaNO}_2$  standard solution, the calibration curve was produced.

### **Determination of $\text{NH}_3$ -N**

The diluted electrolyte was added Potassium sodium tartrate solution (0.1 mL,  $\rho=500$  g/L) and as-prepared Nessler's reagent (0.1 mL). After shaking well, the color was developed for 20 min in dark. UV-Vis spectrophotometry was used to detect the absorbance between the wavelengths of 380 nm and 530 nm. The absorbance at 420 nm is the absorbance of  $\text{NH}_4^+$ -N. The calibration curve is created by measuring the absorbance corresponding to the reference concentration of  $\text{NH}_4\text{Cl}$  solution.

### **$^{15}\text{N}$ Isotope Labeling Experiments**

Isotope labelling experiments using  $\text{K}^{15}\text{NO}_3$  as the raw nitrogen source. Before the  $\text{NO}_3\text{RR}$  test, a

0.5 M K<sub>2</sub>SO<sub>4</sub> electrolyte solution containing 200 mg L<sup>-1</sup> K<sup>15</sup>NO<sub>3</sub>-<sup>15</sup>N was added to the cathode chamber as the reactant. The pH of the tested electrolyte was adjusted to 1-2 with 4 M H<sub>2</sub>SO<sub>4</sub> solution. In order to further quantify the NH<sub>4</sub><sup>+</sup>-N concentration, a standard curve of <sup>15</sup>NH<sub>4</sub><sup>+</sup>-<sup>15</sup>N concentration versus integrated area (<sup>15</sup>NH<sub>4</sub><sup>+</sup>-<sup>15</sup>N/C<sub>4</sub>H<sub>4</sub>O<sub>4</sub>) was obtained using <sup>1</sup>H NMR with maleic acid (C<sub>4</sub>H<sub>4</sub>O<sub>4</sub>) as the external standard. First, different concentrations of <sup>15</sup>NH<sub>4</sub><sup>+</sup>-<sup>15</sup>N (50, 100, 150, 200 and 250 mg L<sup>-1</sup>) were dissolved in 0.5 M K<sub>2</sub>SO<sub>4</sub>, using 120 mg L<sup>-1</sup> C<sub>4</sub>H<sub>4</sub>O<sub>4</sub> as a standard solution. Next, 0.05 mL of deuterium oxide (D<sub>2</sub>O) was mixed with 0.5 mL of the acidified electrolyte or standard solution and the <sup>1</sup>H NMR spectrum was further obtained by nuclear magnetic resonance detection.

Calculation equations of conversion ratio of NO<sub>3</sub><sup>-</sup>, the selectivity of product, the yield rate of NH<sub>4</sub><sup>+</sup> and the Faradaic efficiency (FE):

$$\text{Conversion}_{(\text{NO}_3^-)} = \Delta c_{\text{NO}_3^-} / c_0 \times 100\% \quad (1)$$

$$\text{Selectivity}_{(\text{NH}_4^+)} = c_{\text{NH}_4^+} / \Delta c_{\text{NO}_3^-} \times 100\% \quad (2)$$

$$\text{Yield}_{(\text{NH}_4^+)} = (c_{\text{NH}_4^+} \times V) / (M_{\text{NH}_3} \times t \times S) \quad (3)$$

$$\text{FE} = (8F \times c_{\text{NH}_4^+} \times V) / (M_{\text{NH}_4^+} \times Q) \quad (4)$$

where  $\Delta c_{\text{NO}_3^-}$  is the concentration difference of NO<sub>3</sub><sup>-</sup> before and after reduction,  $c_0$  is the initial concentration of NO<sub>3</sub><sup>-</sup>,  $c_{\text{NH}_4^+}$  is the measured NH<sub>4</sub><sup>+</sup> concentration, V is the electrolyte volume in the cathode chamber (35 mL), t is the electrolysis time (2 h),  $M_{\text{NH}_3}$  is the molar mass of NH<sub>3</sub>, S is the geometric area of working electrode (1 cm<sup>2</sup>), F is the Faraday constant (96485 C mol<sup>-1</sup>), and Q is the total charge during electrolysis.

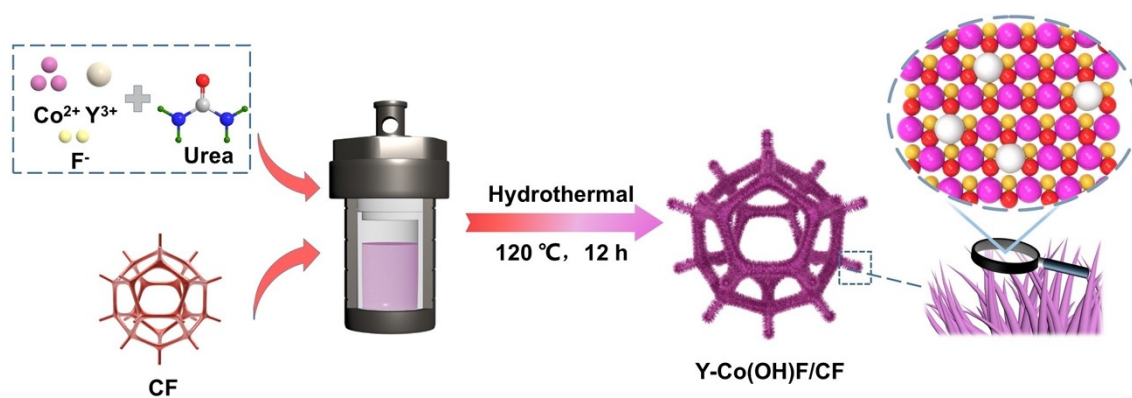


**Fig. S1** Schematic illustration of the synthesis procedures for the Y-Co(OH)F/CF.

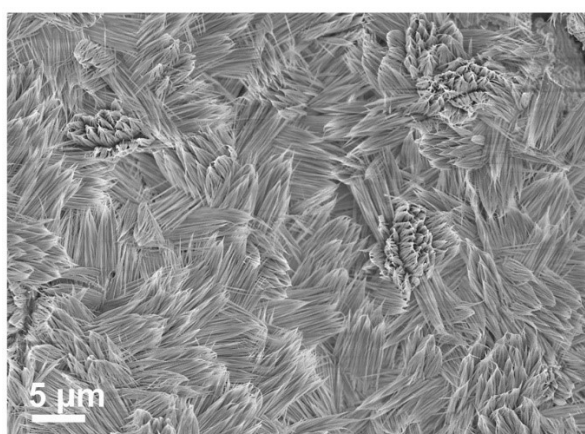


**Fig. S2** SEM image of Co(OH)F/CF.

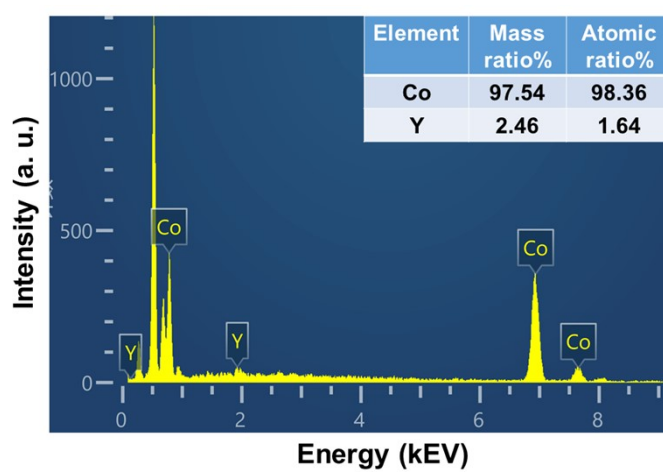


**Fig. S3** EDS spectrum of the Y-Co(OH)F/CF.

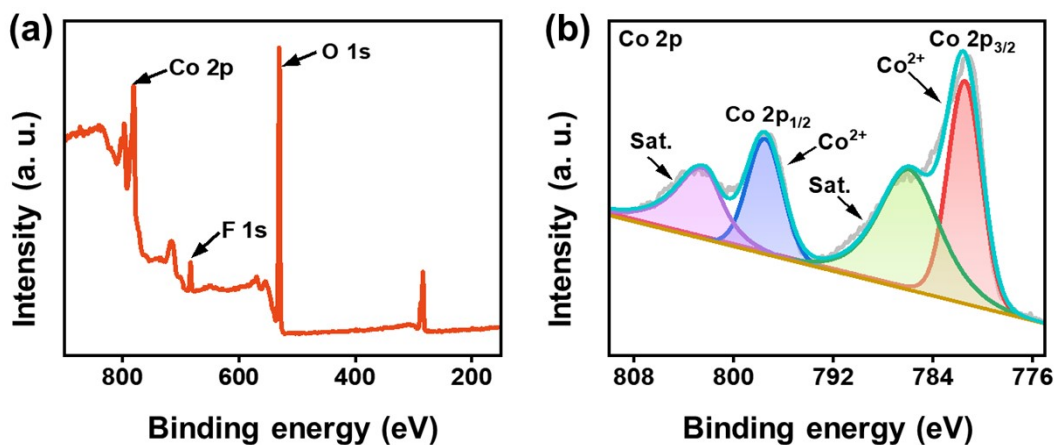


Fig. S4 (a) Full XPS spectrum and (b) high-resolution Co 2p XPS spectrum for Co(OH)F.

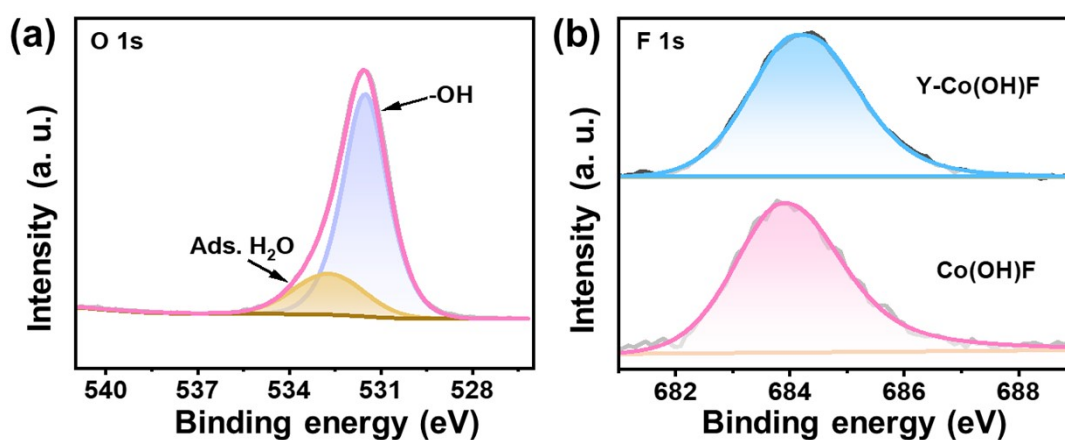


Fig. S5 (a) High-resolution O 1s XPS spectrum for Y-Co(OH)F; (b) High-resolution F 1s XPS spectra for different samples.

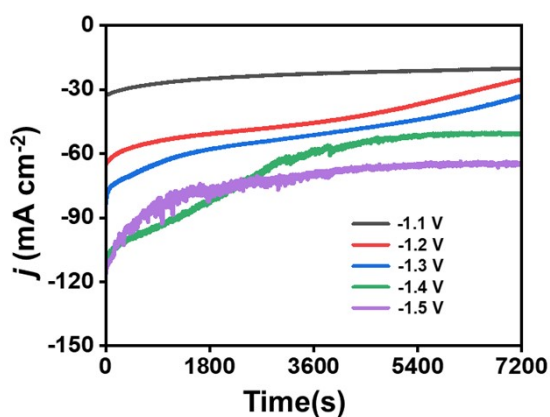
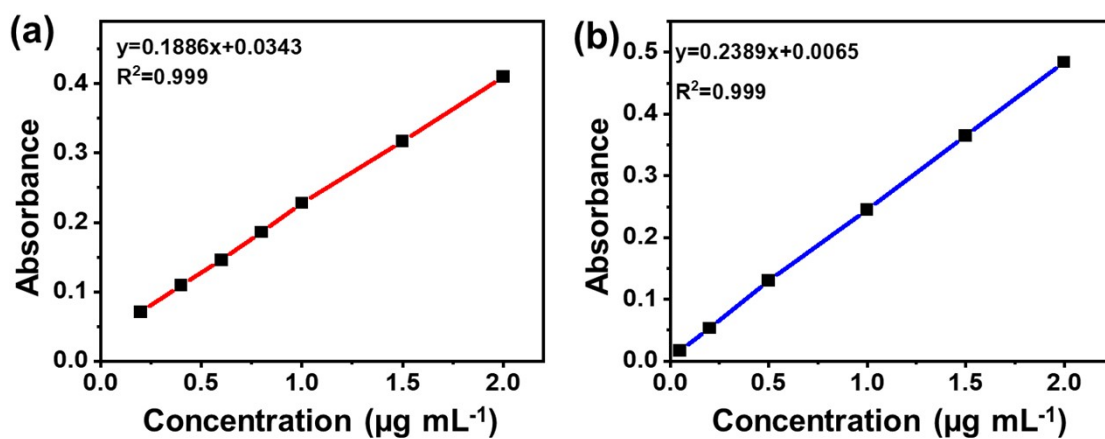
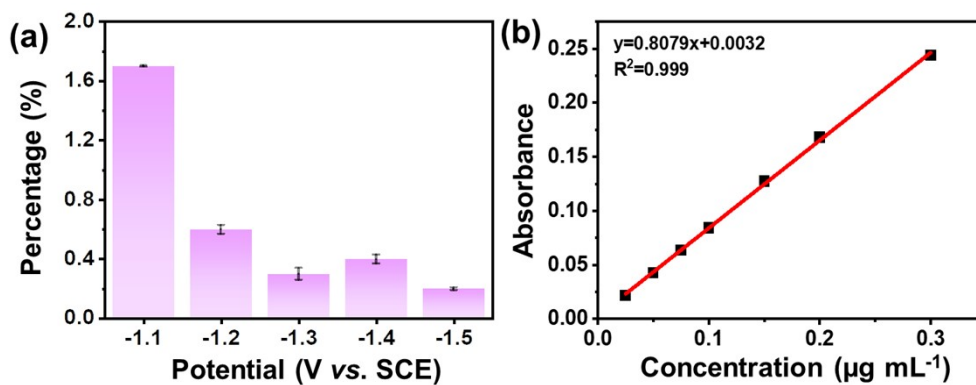


Fig. S6 The i-t curves of the Y-Co(OH)F/CF in 0.5 M K<sub>2</sub>SO<sub>4</sub> with 200 mg L<sup>-1</sup> KNO<sub>3</sub>-N at different potentials.



**Fig. S7** (a) Corresponding calibration curve for calculating the concentration of  $\text{NH}_4^+\text{-N}$ . (b) Corresponding calibration curve for calculating the concentration of  $\text{NO}_3^-\text{-N}$ .



**Fig. S8** (a) Selectivity of  $\text{NO}_2^-\text{-N}$  over the Y-Co(OH)F/CF at different potentials. (b) Calibration curve used to estimate the concentrations  $\text{NO}_2^-\text{-N}$ .

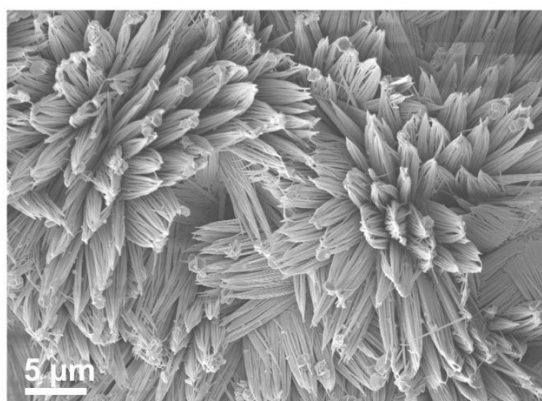


**Fig. S9** SEM image of Y-Co(OH)F/CF after  $\text{NO}_3\text{RR}$  testing.

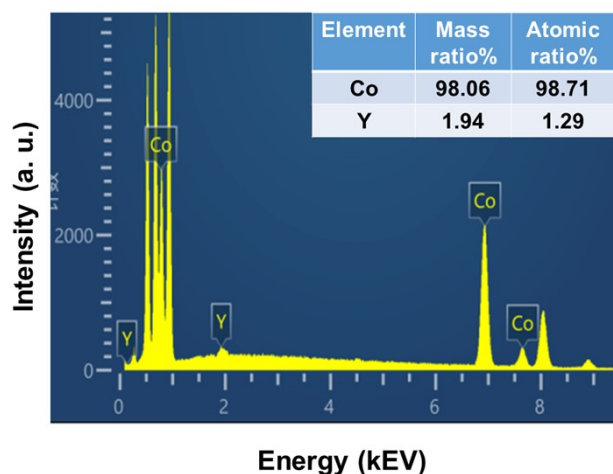


**Fig. S10** EDS spectrum of Y-Co(OH)F/CF after NO<sub>3</sub>RR testing.

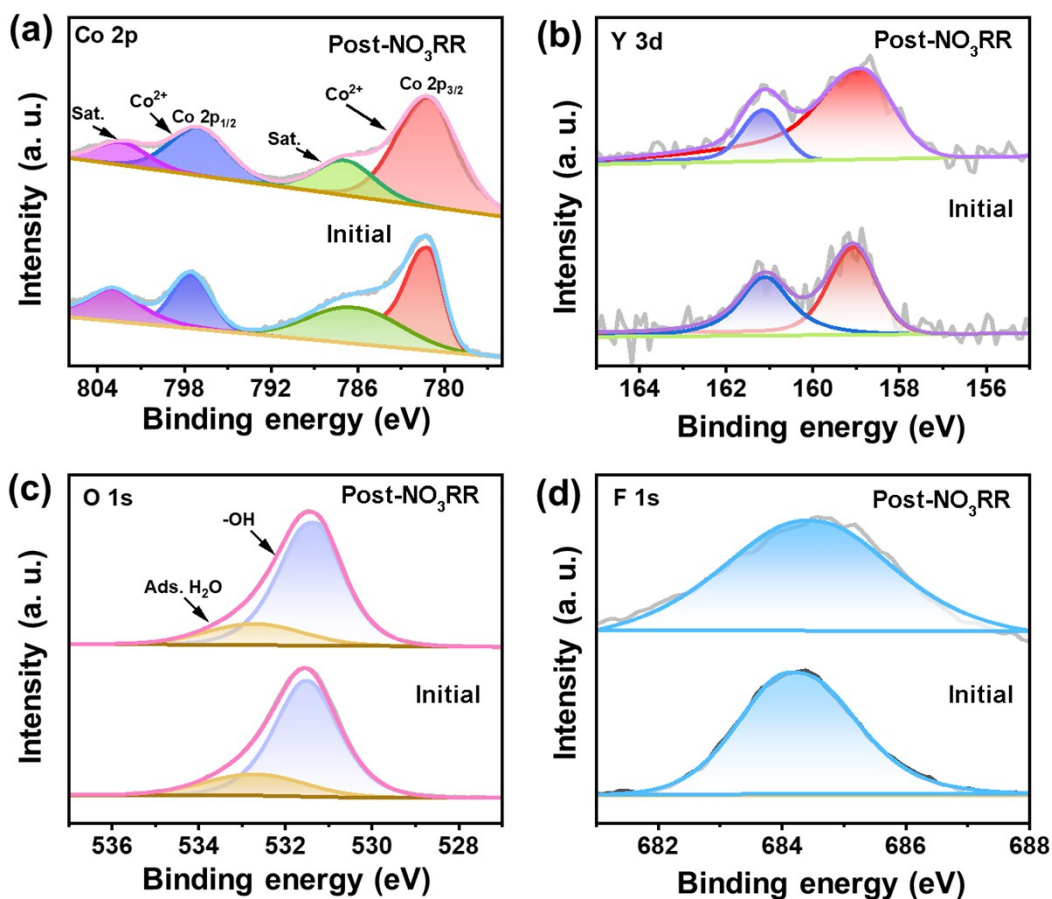


**Fig. R11** (a) High-resolution Co 2p XPS spectra, (b) high-resolution Y 3d XPS spectra, (c) high-resolution O 1s XPS spectra, (d) high-resolution F 1s XPS spectra of Y-Co(OH)F/CF before and after NO<sub>3</sub>RR testing



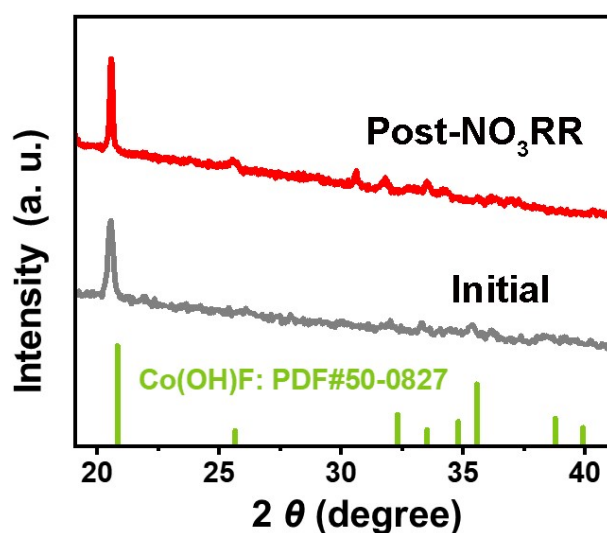


Fig. S12 XRD patterns of Y-Co(OH)F/CF before and after NO<sub>3</sub>RR testing.

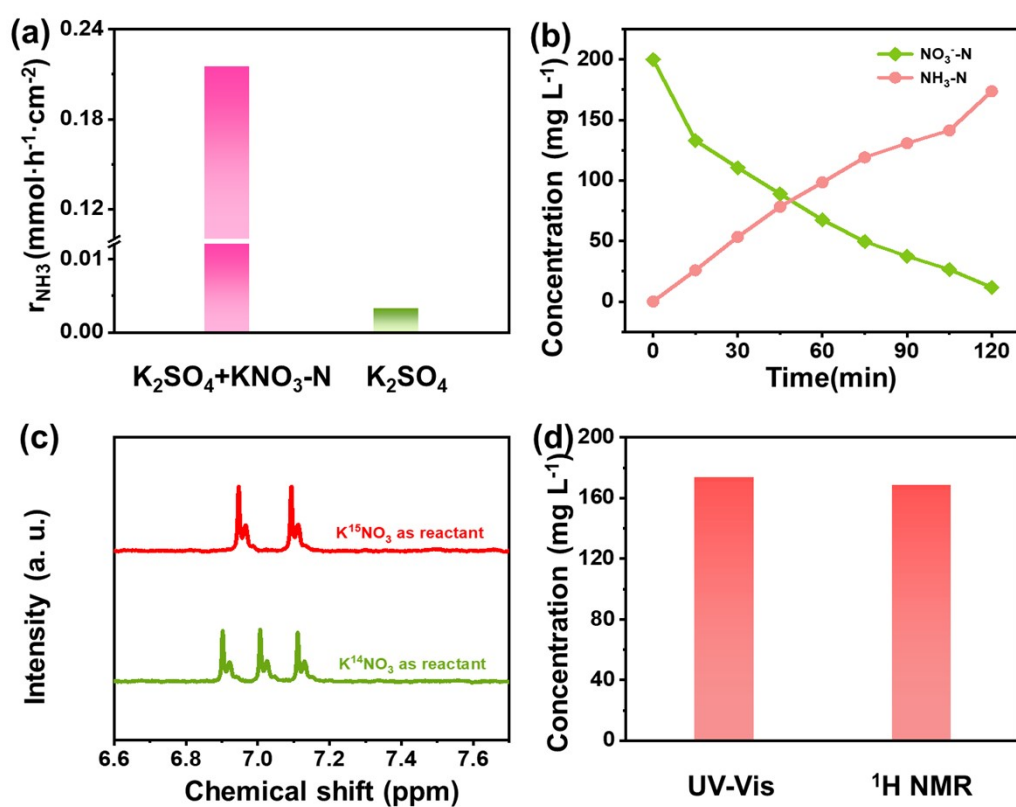
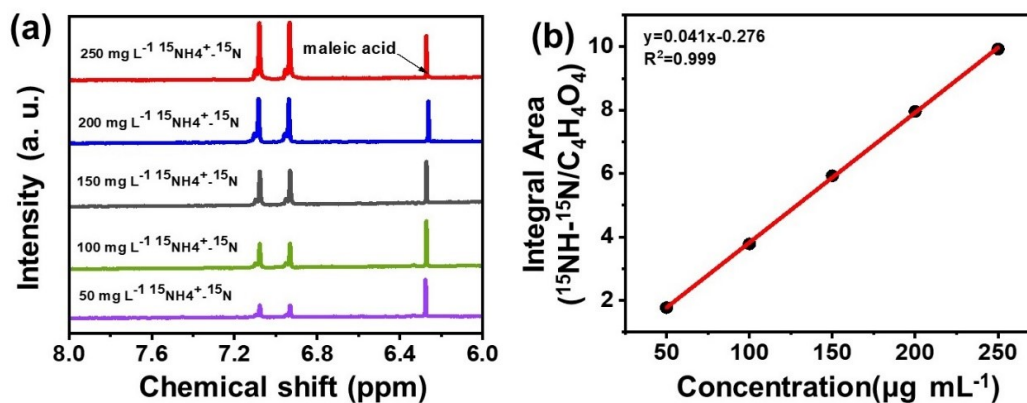
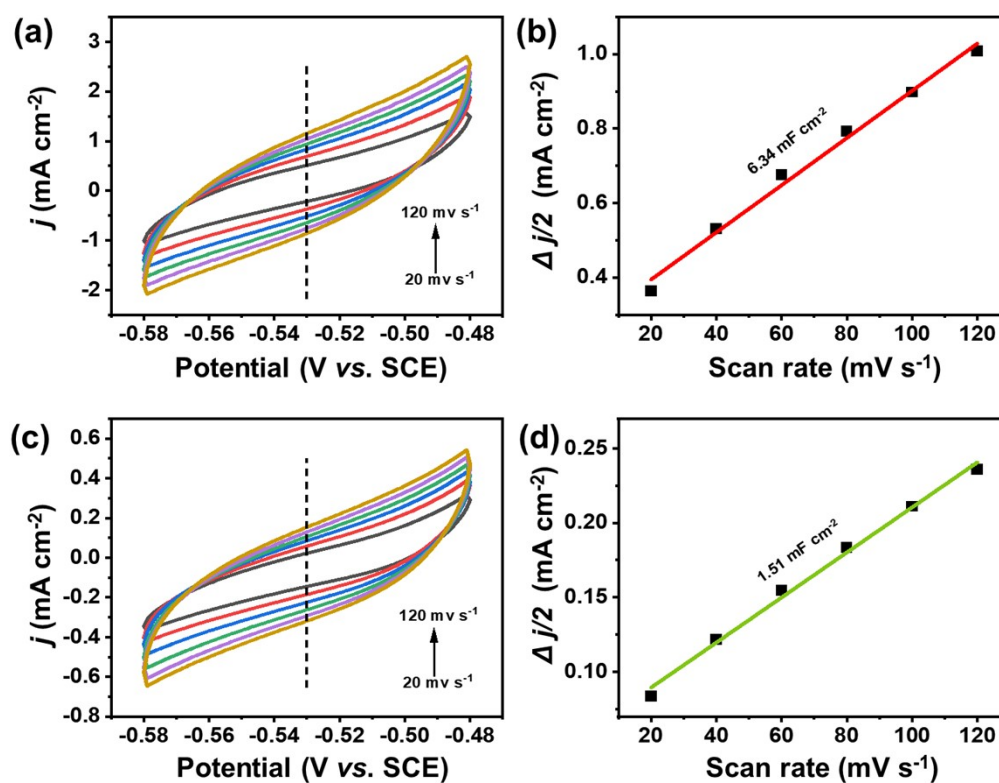


Fig. S13 (a) Yield rates of ammonia from Y-Co(OH)F/CF in a K<sub>2</sub>SO<sub>4</sub> electrolyte with and without nitrate. (b) NO<sub>3</sub><sup>-</sup>-N and NH<sub>3</sub>-N concentrations over the Y-Co(OH)F/CF at -1.3 V vs. SCE change with time. (c) <sup>1</sup>H NMR spectra of the electrolytes after electrolysis using <sup>15</sup>NO<sub>3</sub><sup>-</sup> and <sup>14</sup>NO<sub>3</sub><sup>-</sup> as the nitrogen source. (d) UV-Vis and <sup>1</sup>H NMR measurements of generated NH<sub>3</sub> concentrations using <sup>14</sup>NO<sub>3</sub><sup>-</sup> and <sup>15</sup>NO<sub>3</sub><sup>-</sup> as nitrogen sources.



**Fig. S14** (a)  $^1\text{H}$  NMR spectra of  $^{15}\text{NH}_4^+ \text{-}^{15}\text{N}$  with different concentrations. (b) The standard curve of integral area ( $^{15}\text{NH}_4^+ \text{-}^{15}\text{N}/\text{C}_4\text{H}_4\text{O}_4$ ) against  $^{15}\text{NH}_4^+ \text{-}^{15}\text{N}$  concentration.



**Fig. S15** CV curves of (a) Y-Co(OH)F/CF and (c) Co(OH)F/CF at different scanning rates; Capacitance current densities of (b) Y-Co(OH)F/CF and (d) Co(OH)F/CF at  $-0.53$  V (vs. SCE).

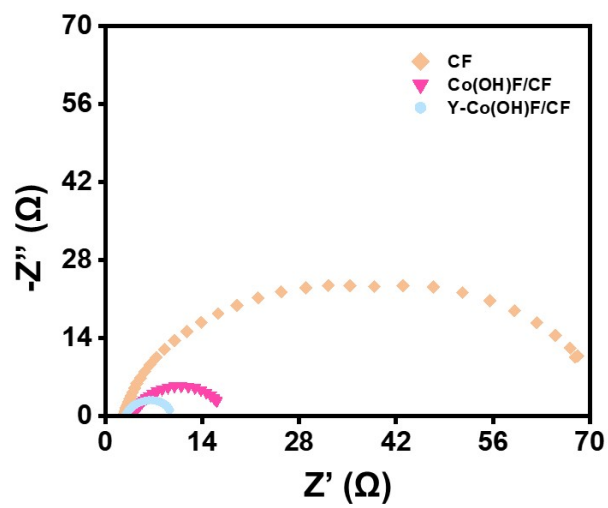


**Fig. S16** EIS spectra of Y-Co(OH)F/CF, Co(OH)F/CF and CF.

**Table S1** Comparison of electrochemical nitrate-to-ammonia performance between the Y-Co(OH)F/CF and some other reported Co-based electrocatalysts.

Electrocatalyst	Electrolyte	Faradaic Efficiency (Potential)	Ref.
Y-Co(OH)F/CF	0.5mol K <sub>2</sub> SO <sub>4</sub> + 200 mg L <sup>-1</sup> KNO <sub>3</sub>	91.81% (-1.3V vs. SCE)	This work
Co <sub>3</sub> O <sub>4</sub> /Ti mesh	0.1 M Na <sub>2</sub> SO <sub>4</sub> + 100 g L <sup>-1</sup> NO <sub>3</sub> <sup>-</sup>	1.23% (2.19 V vs. RHE)	1
Co <sub>3</sub> O <sub>4</sub> @NiO HNTs	0.5mol K <sub>2</sub> SO <sub>4</sub> + 200 mg L <sup>-1</sup> KNO <sub>3</sub>	54.97% (-0.7V vs. RHE)	2
Co/NC-800	0.1 M Na <sub>2</sub> SO <sub>4</sub> + 100 mg L <sup>-1</sup> NO <sub>3</sub> <sup>-</sup>	81.2 % (-1.2 V vs. Ag/AgCl)	3
Co <sub>3</sub> O <sub>4</sub> /CF	50 mM Na <sub>2</sub> SO <sub>4</sub> + 50 mg L <sup>-1</sup> NO <sub>3</sub> <sup>-</sup>	22.19% ( -1.3 V vs. Ag/AgCl)	4
[Bim]NTf <sub>2</sub> -Co <sub>3</sub> O <sub>4-x</sub>	0.1 M Na <sub>2</sub> SO <sub>4</sub> + 500 mg L <sup>-1</sup> KNO <sub>3</sub>	84.74% (-1.41 V vs. Ag/AgCl)	5
PP-Co	0.1 M NaOH + 0.1 M KNO <sub>3</sub>	90.1% (-0.6 V vs. RHE)	6
Co <sub>3</sub> O <sub>4</sub> /Co	0.1 M Na <sub>2</sub> SO <sub>4</sub> + 1 mg mL <sup>-1</sup> NO <sub>3</sub> <sup>-</sup>	88.7% (-0.8 vs. RHE)	7
Co-CuO <sub>x</sub>	500 mg L <sup>-1</sup> Na <sub>2</sub> SO <sub>4</sub> + 144.4 mg L <sup>-1</sup> KNO <sub>3</sub>	53.5%(-1.1 V vs. Ag/AgCl)	8

## References

1. Y. Wang, Y. Yu, R. Jia, C. Zhang and B. Zhang, *Natl. Sci. Rev.*, 2019, **6**, 730-738.
2. Y. Wang, C. Liu, B. Zhang and Y. Yu, *Sci. China Mater.*, 2020, **63**, 2530-2538.
3. H. Liu, J. Qin, J. Mu and B. Liu, *J. Colloid Interface Sci.*, 2023, **636**, 134-140.
4. W. Fu, X. Du, P. Su, Q. Zhang and M. Zhou, *ACS Appl. Mater. Interfaces*, 2021, **13**, 28348-28358.
5. D. Qin, S. Song, Y. Liu, K. Wang, B. Yang and S. Zhang, *Angew. Chem., Int. Ed.*, 2023, **62**.
6. Q. Chen, J. Liang, Q. Liu, K. Dong, L. Yue, P. Wei, Y. Luo, Q. Liu, N. Li, B. Tang, A. A. Alshehri, M. S. Hamdy, Z. Jiang and X. Sun, *Chem. Commun.*, 2022, **58**, 4259-4262.
7. F. Zhao, G. Hai, X. Li, Z. Jiang and H. Wang, *Chem. Eng. J.*, 2023, **461**, 141960.
8. Y. Li, J. Ma, Z. Wu and Z. Wang, *Environ. Sci. Technol.*, 2022, **56**, 8673-8681.